Electronic Supplementary Material (ESI) for Journal of Materials Chemistry A
This journal is © The Royal Society of Chemistry 2013

Electronic Supporting Information

One-pot, large-scale synthesis of magnetic activated carbon nanotubes and their applications for arsenic removal

Jie Ma[a], Zhiliang Zhu[a], Bo Chen[a], Mingxuan Yang[a], Huiming Zhou[a], Chen Li[a], Fei Yu[a,b]*, Junhong Chen[a,c]*

[a] State Key Laboratory of Pollution Control and Resource Reuse, School of Environmental Science and Engineering, Tongji University, 1239 Siping Road, Shanghai 200092, China

[b] School of Environmental Science and Engineering, Shanghai Jiao Tong University, 800 Dong Chuan Road, Shanghai 200240, China

[c] Department of Mechanical Engineering, University of Wisconsin–Milwaukee, Milwaukee, WI 53211, USA

Materials and methods

Preparation of MI/CNTs composites.

The MI/CNTs composites were prepared by a alkali-activated method using APCNTs. The APCNTs were prepared by the catalytic chemical vapor deposition method[1]. In a typical synthesis, APCNTs and KOH powder were mixed in a stainless steel vessel in an inter-gas atmosphere. The weight ratio of KOH to APCNTs was 1:4. The APCNTs and KOH powder was mixed for 10 min using a mortar, which resulted in a uniformly powder mixture. The mixture was then heated to 1023 K for 1 h under flowing argon in a horizontal tube furnace, washed in the deionized water, and then dried.

Characterization methods

The microstructure and morphology of the APCNTs or MI/CNTs composites was analyzed by transmission electron microscopy (TEM, JEOL 2100, Japan). X-Ray diffraction (XRD) experiments were conducted on specimens of the magnetic hybrid materials; the X-ray diffractometer (Bruker D8 Advance, Bruker AXS, Germany) was operated at 40 KV and 40 mA. Nickel-filtered Cu_{Ka} radiation was used in the incident

beam. The specific surface area, pore volume, and pore size distribution of the MI/CNTs composites were calculated from the adsorption/ desorption isotherms of N_2 at 77K by the multi-point BET and DFT method using an Autosorb-iQ-C (Quantachrome, American, Inc.), and the sample was degassed at 373k for 4h prior to the measurements. X-Ray photoelectron spectroscopy (XPS) analysis was carried out in a Kratos Axis Ultra DLD spectrometer, using monochromated Al Ka X-rays at a base pressure of 1×10^{-9} Torr. Survey scans determined between 1100 and 0 eV revealed the overall elemental compositions of the sample, and regional scans for specific elements were performed. The peak energies were calibrated by placing the major C_{1s} peak at 284.6 eV. Samples were prepared identically to those of the batch experiments. Raman spectroscopy (JOBIN-YVON T64000) was used to further characterize MI/CNTs. A TA Instruments® Q600 SDT thermal analyzer was used for high-resolution thermogravimetric analysis (TG) and differential thermal analysis (DTA). TG and DTA curves were obtained by heating approximately 10 mg of MI/CNTs from 50 to 900°C at a heating rate of 10 °C/min in air. The magnetization was measured using a superconducting quantum interference device magnetometer (MPMS XL7, Quantum Design). The residual As(V) and As(III) concentrations in solution were determined by an Inductively Coupled Plasma Optical Emission Spectrometry (ICP-OES, Optima 2000, Perkin Elmer, U.K.).

Batch sorption experiments

Batch experiments were conducted to evaluate the adsorption performance of As(V) or As(III) on the adsorbents. Two typical materials, APCNTs and MI/CNTs, were selected as adsorbents for As(V) or As(III) adsorption in an aqueous solution. 1000 $mg\cdot L^{-1}$ Stock solution of As (V) and As(III) was prepared by dissolving 4.1653 g $Na_2HAsO_4\cdot7H_2O$ and 1.732 g $NaAsO_2$, respectively, in 1L deionized water. And working solutions of required concentrations were obtained by diluting the As(V) and As(III) stock solution with deionized water. All the sorption tests were conducted in well-capped 250 mL flasks containing 50 mL As(V) or As(III) solution with required concentration. After 10 mg of adsorbent was added, the flasks were shaken in a thermostatic shaker at 150 rpm at 298K for 24 h. All the adsorption experiments were

conducted in duplicate, and only the mean values were reported. The maximum deviation for the duplicates was usually less than 5%. The blank experiments without the addition of APCNTs or MI/CNTs were conducted to ensure that the decrease in the concentration was actually due to the adsorption of APCNTs or MI/CNTs, rather than by the adsorption on the glass bottle wall. After adsorption, the adsorbent was separated by a 0.45μm membrane. The residual arsenic concentrations in solution were determined by an Inductively Coupled Plasma Optical Emission Spectrometry (ICP-OES, Agilent 720ES, USA). The adsorption isotherm was studied at pH 5.5，the initial concentration of As(V) or As(III) solution was set from 0.5 mg/L to 11 mg/L, and the adsorption isotherms were then modeled using the Langmuir, Freundlich, and Dubinin-Radushkevich (D-R) isothermal adsorption model.

The amount of adsorbed As(V) or As(III) on adsorbents (q_t, mg/g) was calculated as follows:

$$q_t = (C_0 - C_t) \times \frac{V}{m} \qquad (1),$$

Where c_0 and c_t are the As(V) or As(III) concentrations at the beginning and after a period of time (mg/L); V is the initial solution volume (L); and m is the adsorbent weight (g).

UV-Visible Spectroscopy

Measurements were made on the CNTs solution in quartz cuvettes using a double-beam UV-visible spectrophotometer(UV759UV-VIS, Shanghai Precision & Scientific Instrument Co. Ltd.) in the 200-800 nm range. Since the Beer-Lambert law is not obeyed at strong absorbance[2], the CNTs solution were diluted appropriately to keep the measured values of absorbance in the range of 0.1-2 in the entire wavelength range[3]. A UV-visible absorption-based approach is used for a direct measurement of the concentration of CNTs[4, 5]. A calibration plot is then made by monitoring the intensity of the peak as a function of the true concentration of the CNTs. Earlier reference stated that the adsorption peak at ~265 nm is a signature of the surface π-plasmon exciation of the CNTs. Thus, we build a calibration curve by monitoring

the adsorbance value for this peak at 265 nm as a funciton of CNT concentration, and then we are able to estimate the unknown concentration of CNTs in the solution by measuring its optical absorbance.

Data analysis

Langmuir model

The form of the Langmuir isotherm can be represented by the following equation:

$$q_e = q_m \frac{K_L C}{1 + K_L C} \qquad (2)$$

where q_e is the amount of dye adsorbed per gram of adsorbent (mg/g), C denotes the equilibrium concentration of dye in solution (mg/L); K_L represents the Langmuir constant (L/mg) that relates to the affinity of binding sites; and q_m is a theoretical limiting adsorption capacity when the monolayer surface is fully covered with dye molecules and assists in the comparison of adsorption performance (mg/g). Another important parameter, R_L (the separation factor or equilibrium parameter, which can be used to determine the feasibility of adsorption in a given concentration range over adsorbent), also evaluated in this study, was determined from the relation[6]:

$$R_L = \frac{1}{1 + K_L C_0} \qquad (3)$$

where K_L is the Langmuir adsorption constant (l/mg) and C_0 is the initial dye concentration (20mg/l). Ho and McKay[7] established that (1) $0<R_L<1$ for favorable adsorption, (2) $R_L>1$ for unfavorable adsorption, (3) $R_L=1$ for linear adsorption and (4) $R_L=0$ for irreversible adsorption.

Freundlich model

The Freundlich isotherm model has the following form:

$$q_e = K_F C^{1/n} \qquad (4)$$

where q_e is the amount of dye adsorbed per gram of adsorbent (mg/g); C is the equilibrium dye concentration in solution (mg/L); K_F and n are the Freundlich

constants, which represent the adsorption capacity and the adsorption strength, respectively. The magnitude of *1/n* quantifies the favorability of adsorption and the degree of heterogeneity of the adsorbent surface.

Dubinin-Radushkevich (D-R) model

The D-R isotherm model has the following form:

$$\ln q_e = \ln q_m - B\varepsilon^2 \qquad (5)$$

B, a constant related to the mean free energy of adsorption (mol^2/kJ^2); q_m, the theoretical saturation capacity; and ε, the Polanyi potential, which is equal to

$$\varepsilon = RT\ln(1+\frac{1}{C}) \qquad (6)$$

where *R* ($J\cdot mol^{-1}\cdot K^{-1}$) is the gas constant and *T* (K) is the absolute temperature. For the D-R isotherm model, from *B* values the mean energy of adsorption, *E*, can be calculated using the relation[8]

$$E = \frac{1}{\sqrt{-2B}} \qquad (7)$$

Based on equations (5), (6), and (7), the isotherm constants, *E* and determination coefficients were calculated. The mean energy of adsorption (E) is the free energy change when one mole of ions is transferred from infinity in the solution to the surface of the solid. When one mole of ions is transferred, its value is in the range of 1-8 $kJ\cdot mol^{-1}$ for physical adsorption[9]. The value of E is between 8 and 16 $kJ\cdot mol^{-1}$ for an adsorption process by ion-exchange. A value of E in the range of 20-40 $kJ\cdot mol^{-1}$ is indicative of chemisorption[10].

This journal is © The Royal Society of Chemistry 2013

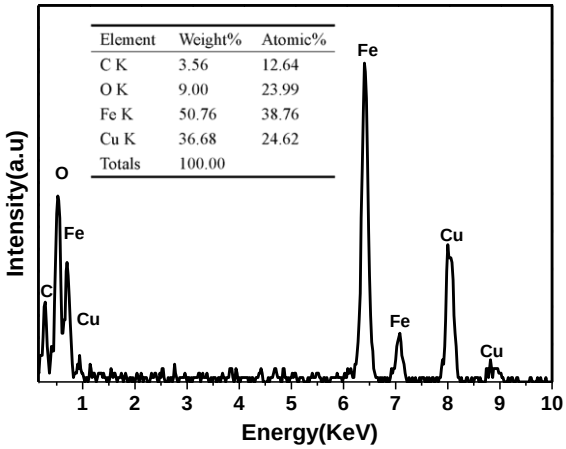

Fig. S1 EDS of MI/CNTs.

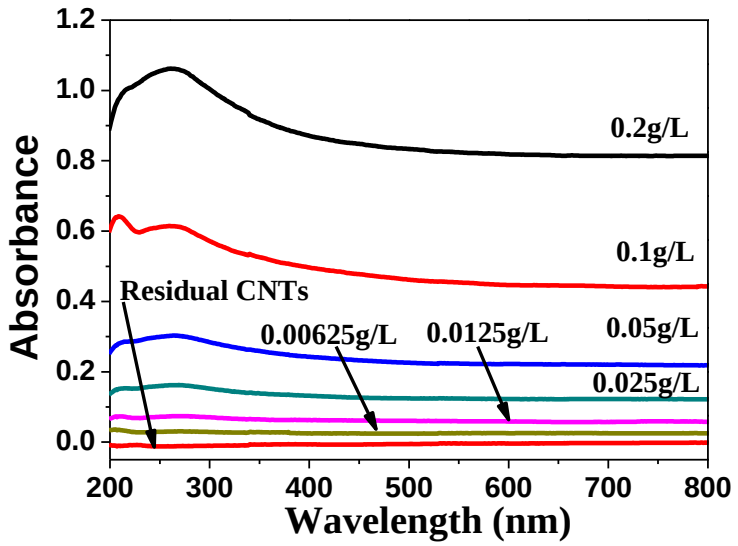

Fig S2 Representative absorption spectra of CNTs in aqueous solution with different concentration

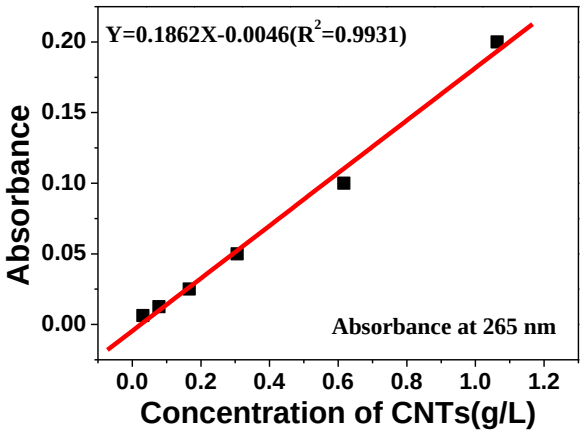

Fig. S3 Absorbance of CNT dispersion with varying concentration

Fig. S3 shows a plot of absorbance at 265 nm, measured as a function of CNT concentration. While the intensity of the 265 nm peak increases linearly with increasing CNT concentration. Thus, the intensity of the 265 nm peak could be used in the construction of the calibration plots for the true CNT concentration. The linear calibration curves show the true concnetration of CNTs in the given dispersion (in agreement with Beer-lambert law). With these curves in hand, we are able to estimate the real concentration of residual CNTs in an aqueous dispersion after magnetic separation. In this procedure, the absorbance of the CNTs dispersion after magnetic separation is measured and the CNT concentration is determined from the calibration curve. The adsorbance of the residual CNTs is -0.007, as shown in Fig. S2. It is noteworthy to observe that the conocentration of residual CNTs is almost 0 g/L, calculated from the linear calibration curves, as shown in Fig. S3.

This journal is © The Royal Society of Chemistry 2013

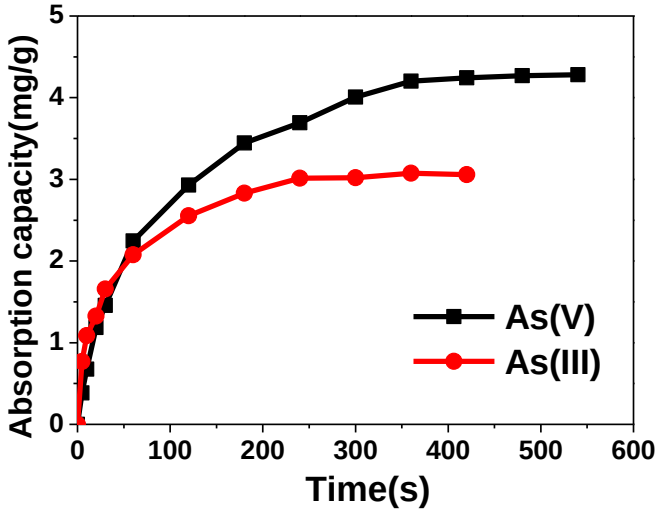

Fig. S4 Kinetic curves of arsenic removal on MI/CNTs (As(V)/As(III) concentration=2 mg/L, MI/CNTs=0.2 g/L)

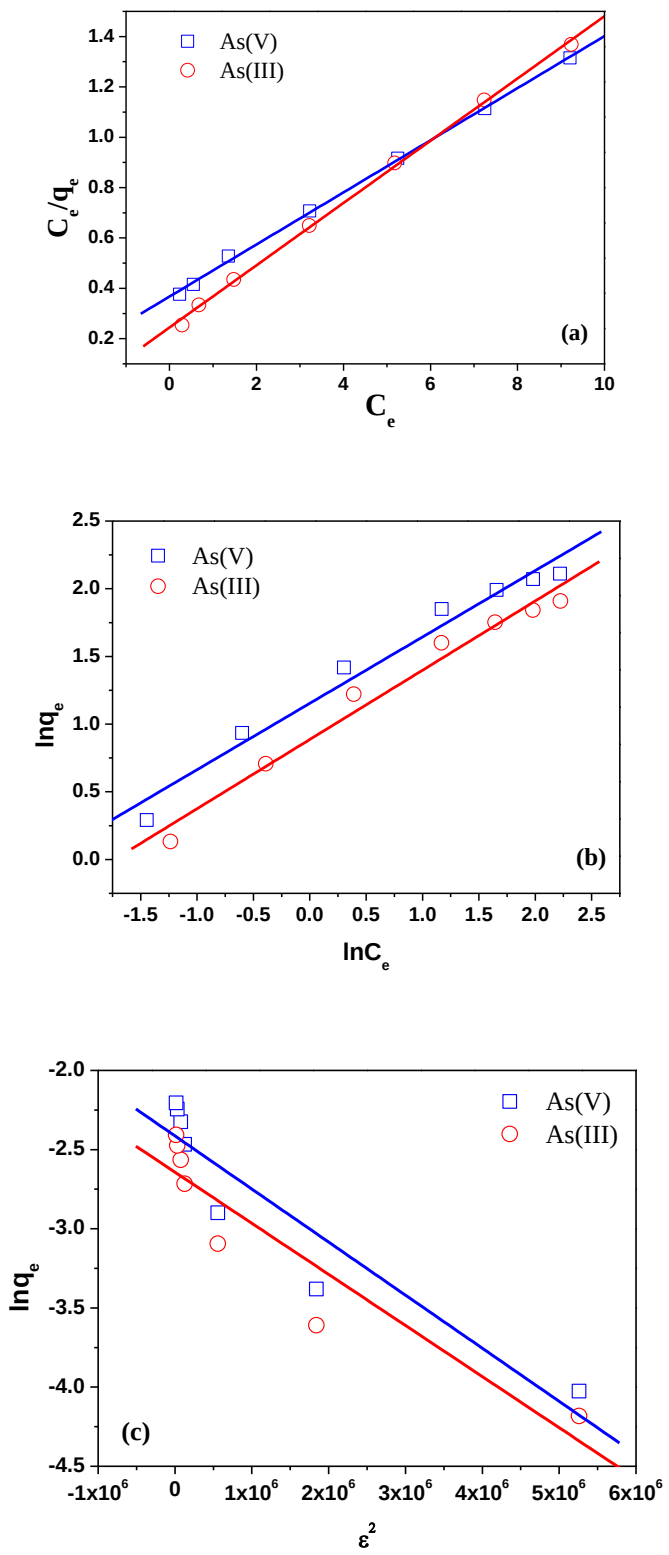

Fig. S5 (a) Langmuir, (b) Freundlich, (c) D–R isotherms for As(V) and As(III) adsorption onto MI/CNTs.

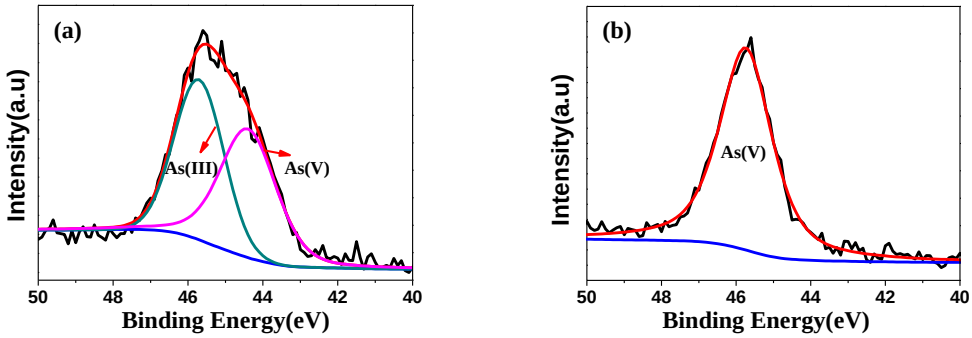

Fig. S6 As 3d XPS spectra of MI/CNTs after As(III) (a) and As(V) (b) adsorption

This journal is © The Royal Society of Chemistry 2013

Table S1 Physical properties of APCNTs and MI/CNTs

Adsorbents	Surface area (m^2/g)			Average pore size	Pore volume	Pore volume(cm^3/g)		
	SSA	ESA	ISA	nm	cm^3/g	Micropore	Mesopore	Macropore
APCNTs	113.5	127.5	0	11.03	2.004	0.048	0.305	1.651
MI/CNTs	662.1	617.8	44.3	2.26	0.726	0.275	0.451	0.037

This journal is © The Royal Society of Chemistry 2013

Table S2 Atomic ratios of element in APCNTs and MI/CNTs

Adsorbents	C%	O%	Fe%	As%
APCNTs	96.72	2.88	0.4	0
MI/CNTs	72.36	21.06	6.58	0
MI/CNTs-As(III)	78.97	15	5.35	0.68
MI/CNTs-As(V)	75.45	18.13	5.86	0.56

This journal is © The Royal Society of Chemistry 2013

Table S3. Langmuir, Freundlich, and Dubinin-Radushkevich isotherms parameters of As(V) and As(III) adsorption on MI/CNTs system

Adsorbate	Langmuir model			Freundlich model			Dubinin-Radushkevich model			
	q_m(mg/g)	K_L(l/mg)	R^2	K_F	n	R^2	B(mol/kJ^2)	Q_m(mg/g)	E(kJ/mol)	R^2
As(V)	9.74	0.589	0.998	3.54	2.44	0.967	4E-7	10.02	1118	0.463
As(III)	8.13	0.490	0.999	2.70	2.31	0.971	4E-7	8.28	1118	0.417

Reference

[1] J. Ma, J.N. Wang, X.X. Wang, J Mater Chem 19 (2009) 3033.

[2] J.F. Offersgaard, H. Ojelund, Appl Spectrosc 56 (2002) 469.

[3] J.L. Bahr, E.T. Mickelson, M.J. Bronikowski, R.E. Smalley, J.M. Tour, Chem Commun (2001) 193.

[4] S. Attal, R. Thiruvengadathan, O. Regev, Anal Chem 78 (2006) 8098.

[5] S.H. Jeong, K.K. Kim, S.J. Jeong, K.H. An, S.H. Lee, Y.H. Lee, Synthetic Met 157 (2007) 570.

[6] G.H. Sonawane, V.S. Shrivastava, Desalin Water Treat 29 (2011) 29.

[7] Y.S. Ho, G. McKay, Chem Eng J 70 (1998) 115.

[8] J.P. Hobson, J. Phys. Chem. 73 (1969) 2720.

[9] M.S. Onyango, Y. Kojima, O. Aoyi, E.C. Bernardo, H. Matsuda, J Colloid Interf Sci 279 (2004) 341.

[10] S.S. Tahir, N. Rauf, Chemosphere 63 (2006) 1842.